

## Assessing the Impact of Proposed Regulator's Construction on Water Quality of Shatt Al-Arab River-Iraq

Mohammed Jabbar Mawat  \*, Ahmed Naseh Ahmed Hamdan  

Department of Civil Engineering, College of Engineering, University of Basrah, Basrah, Iraq

### ABSTRACT

The Shatt Al-Arab River, in southern Iraq, flows southeastwards through Basrah City to the Arabian Gulf. Seven creeks are branched off the river: Jubyla, Muftya, Robot, Khandek, Ashar, Khora, and Saraji, where they are affected by tidal phenomena. The change in the hydrological status of the river over the last decade has adversely affected the quality of the river's water. Urban sewage and industrial wastewater are usually discharged directly or indirectly into the river. The entire river's course is studied, starting at the point where the Tigris and Euphrates rivers meet in the Qurnah district and extending into the vicinity of the river's estuary. The use of the Shatt Al Arab River in modelling a planned regulator on the river is demonstrated as one of the solutions offered to address the deterioration of river water quality. Results showed a slight increase in organic nitrogen, nitrate, ammonia, organic phosphorus, inorganic phosphorus, and carbonaceous biochemical oxygen demand by (4.76, 3.61, 7.23, 4.44, 2.76, and 12.27%), respectively, and a decrease in dissolved oxygen by 2.6% were because of trapping pollutants fed by rivers branches and cleaning process stopping that was caused by the tides. This increase is expected. It does not cause significant harm compared to the benefit expected from constructing the regulator because of the high decrease in total dissolved solids by 30.58% and phytoplankton by 80.7%. In addition, there are government efforts to prevent this pollution by establishing a system of conveyor pipelines to get rid of these pollutants. It is concluded that there is a great benefit to establishing a regulator.

**Keywords:** HEC-RAS, Proposed regulator, Shatt Al Arab river modeling, Water quality.

---

\*Corresponding author

Peer review under the responsibility of University of Baghdad.

<https://doi.org/10.31026/j.eng.2024.08.07>



This is an open access article under the CC BY 4 license (<http://creativecommons.org/licenses/by/4.0/>).

Article received: 21/09/2023

Article revised: 10/12/2023

Article accepted: 13/12/2023

Article published: 01/08/2024



## 1. INTRODUCTION

The Shatt Al-Arab River (SAR) has significant importance since it facilitates agricultural productivity within a region characterized by aridity and a hot, humid environment (**Al-Ansari et al., 2014; Hamdan et al., 2018**). The water system of SAR is now under increasing strain, both in terms of water quantity and quality (**Abd-El-Mooty et al., 2016; Abdullah et al., 2015; Al-Imara et al., 2013**). The demand for freshwater has been a significant surge, mostly because of the fast growth of the population in Iraq. The increased water allocation for various human activities exerted pressure on existing freshwater resources and water quality (**Abdullah, 2017; Mohammed and Al Chalabi, 2022**). SAR is primarily fed by four main tributaries: the Tigris, Euphrates, Karkheh, and Karun Rivers (**Al-Asadi, 2017; Al-Asadi and Alhello, 2019**). Presently, the contributions have experienced a decrease due to the implementation of strategies by neighbouring countries. Furthermore, it is essential to acknowledge that the water resource policies adopted in Iraq had a cumulative impact on the issue above. Specifically, in 2009, the situation was worse when procedures were taken to split the Euphrates River entrance into SAR. This was achieved by the construction of an embankment along the stream, situated roughly 35 km west of the Al-Qurnah region. (**Lafta, 2022; Najm, 2017**). The purpose of this process is to reduce the salinity of SAR. In recent years, most of SAR water has come only from the Tigris River (**Al-Asadi and Abdullah, 2015**). SAR's hydrological conditions have considerably altered in the past ten years, leading to detrimental consequences for the river's water quality. Total Dissolved Solid (TDS) levels in SAR are increased due primarily to the intrusion of saline water from the Arabian Gulf (**Yaseen et al., 2016; Abdullah et al., 2016a; Abdullah et al., 2016b; Mohamed and Abood, 2017**). SAR has several environmental difficulties, encompassing the contamination resulting from oil spills, agricultural runoff, and sewage discharge (**AL-Amiri and Disher, 2020; Al-Asadi et al., 2020; Alkanany et al., 2017; Lateef et al., 2020**). Water quality is one of the most pressing issues affecting SAR (**Al-Asadi et al., 2022; Mujtaba et al., 2021**). Usually, urban sewage and industrial wastewater are discharged directly into the rivers or their branches through discharge pipes or channels at selected locations. The construction of a regulator on SAR is one of the solutions offered to preserve the freshwater fed from the Tigris River, which reduces the salt intrusion coming from the Arabian Gulf and controls the salt levels within the province of Basrah. This procedure helps to enable the optimal use of water releases for various aspects of life. (**Hamdan et al., 2019**) simulated the impact of a proposed regulator on SAR using the HEC-RAS model. The results encourage the construction of the regulator, considering certain precautions. (**Ali and Al Thamiry, 2021**) used a one-dimensional unsteady model to study the hydraulic effects of a proposed barrage near Ras Al-Besha on SAR. The studied discharges substantially impacted the depths required for navigation, with increasing sediment levels in barrage locations due to the decreasing flow velocity. (**AlKhafaji et al., 2023**) tested a proposed inflatable rubber dam for feasibility and suitability on SAR and compared it with other hydraulic structure regulators.

This investigation aims to describe the hydrodynamics of SAR and the transportation of contaminants along it using the HEC-RAS software by applying a 2D comprehensive model. This model will simulate the establishment of the regulator and suggest the appropriate location to reach the desired result while ensuring the possibility of flood control in the event

of increased water releases from U/S and finding logical solutions to avoid flooding in the case of high discharge from U/S.

## 2. MATERIAL AND METHODS

### 2.1 Description Of Study Area

The Tigris and Euphrates Rivers meet near Al- Qurna district in southern Iraq to form the Shatt al-Arab River (**Fig. 1**).

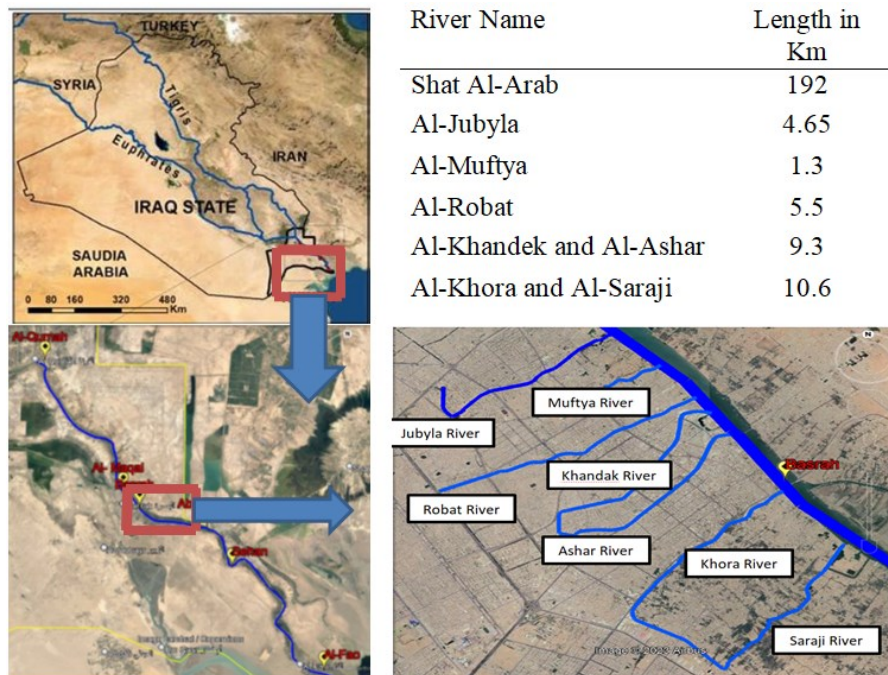


**Figure 1.** Shatt Al-Arab River and its main branches

The Shatt al-Arab River is a 192-kilometer-length tidal river that flows south-east wards, passing through Basrah and then discharging into the Arabian Gulf. The province's seven creeks (Jubyla, Muftya, Robat, Khandek, Ashar, Khora, and Saraji) are linked to the Shatt al-Arab River and are affected by the tidal phenomenon. The river's width changes along its length, from 250 to 300 meters at the Euphrates-Tigris meet. They reach 600 meters around Basrah and 2000 meters at the estuary (**Hamdan, 2015**). The last 95 kilometers of its course, the river forms part of the border between Iraq and Iran (**Abdullah, 2016**).

### 2.2 Model Governing Equations

The area of investigation, SAR, may be classified as a shallow water body due to its width-to-depth ratio exceeding 10 (**Al-Azzawi and Khudair, 2001; Krenkel, 2012**). Consequently, a depth-averaged two-dimensional hydrodynamic model is implemented to simulate the changes of hydraulic parameters in a horizontal plane, including both the longitudinal and



transverse directions, within the HEC-RAS software. The following equations represent the 2-D Shallow-Water equations: continuity and momentum (Abdo, 2014; Mawat and Hamdan, 2023b; Munoz, 2017).

$$\frac{\partial h}{\partial t} + \frac{\partial(Hu)}{\partial x} + \frac{\partial(Hv)}{\partial y} = q \quad (1)$$

$$\frac{\partial u}{\partial t} + u \frac{\partial u}{\partial x} + v \frac{\partial u}{\partial y} - f_c v = -g \frac{\partial h}{\partial x} + \frac{1}{H} \frac{\partial}{\partial x} \left( v_{t,xx} H \frac{\partial u}{\partial x} \right) + \frac{1}{H} \frac{\partial}{\partial y} \left( v_{t,yy} H \frac{\partial u}{\partial y} \right) - \frac{\tau_{b,x}}{\rho R} - \frac{\tau_{s,x}}{\rho H} \quad (2)$$

$$\frac{\partial v}{\partial t} + u \frac{\partial v}{\partial x} + v \frac{\partial v}{\partial y} + f_c u = -g \frac{\partial h}{\partial y} + \frac{1}{H} \frac{\partial}{\partial x} \left( v_{t,xx} H \frac{\partial v}{\partial x} \right) + \frac{1}{H} \frac{\partial}{\partial y} \left( v_{t,yy} H \frac{\partial v}{\partial y} \right) - \frac{\tau_{b,y}}{\rho R} - \frac{\tau_{s,y}}{\rho H} \quad (3)$$

The variable "t" represents time in day, while "H" represents the water depth in meter. The variables "u" and "v" represent the velocity components in the x and y directions in m/s, respectively. The variable "q" is the source/sink flux term in mg/l, where negative values indicate sinks and positive values indicate sources. The variable "g" represents the acceleration of gravity in m/s<sup>2</sup>, while "h" represents the elevation of the water surface in meter. The horizontal eddy viscosity coefficients in the x and y directions are denoted as  $v_{t,xx}$  and  $v_{t,yy}$  Pa.s, bottom shear stresses on the x and y directions are represented by  $\tau_{b,x}$  and  $\tau_{b,y}$ ,  $\tau_{s,x}$  and  $\tau_{s,y}$  represent the surface wind stresses directions N/m<sup>2</sup>, R is the hydraulic radius in metre, and  $f_c$  is the Coriolis parameter.

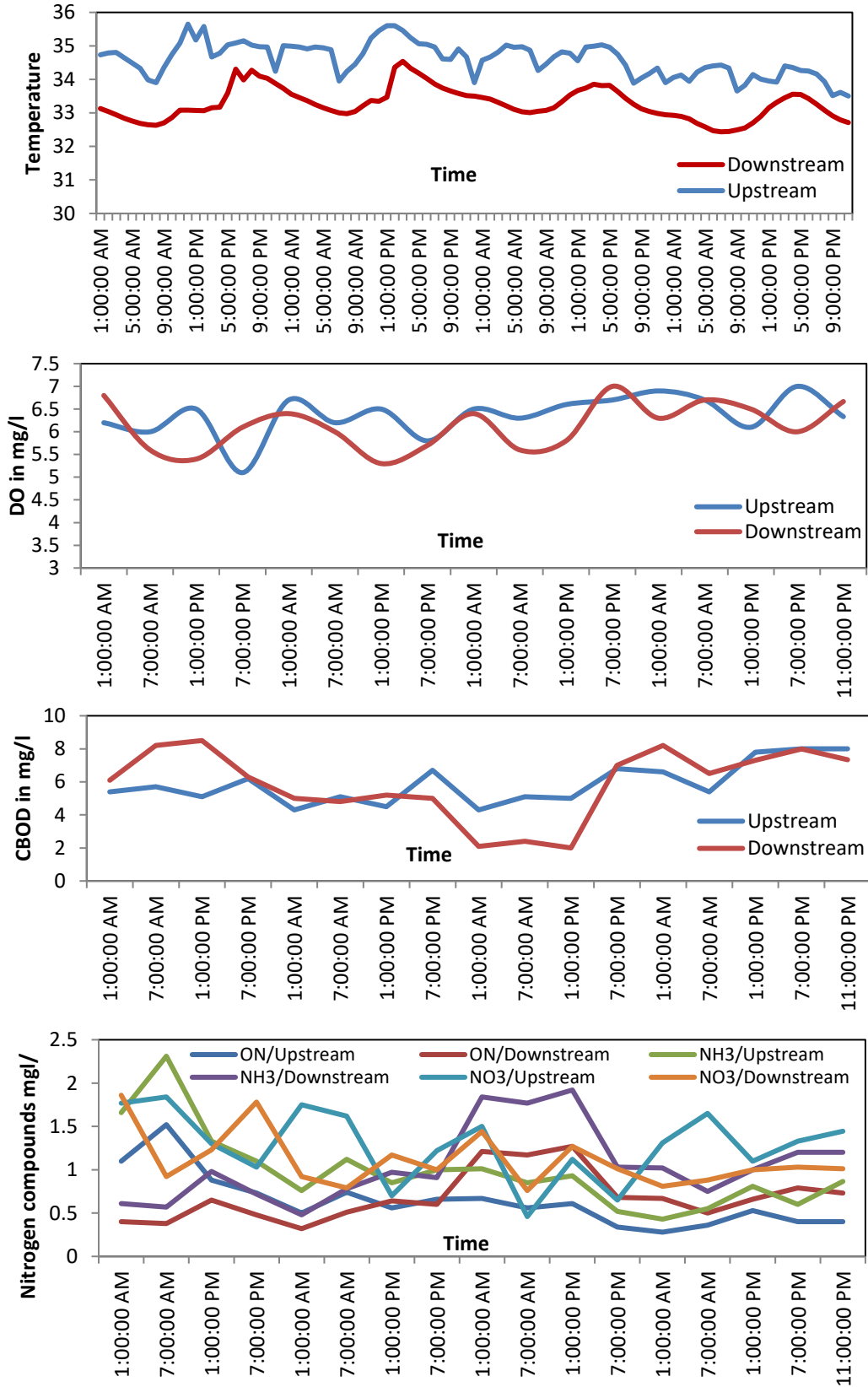
In WASP, the 2D mass transport equation is (Mawat and Hamdan, 2023a; Wool et al., 2020):

$$\frac{\partial(HC)}{\partial t} + \frac{\partial(uHC)}{\partial x} + \frac{\partial(vHC)}{\partial y} = \frac{\partial}{\partial x} \left( HE_x \frac{\partial C}{\partial x} \right) + \frac{\partial}{\partial y} \left( HE_y \frac{\partial C}{\partial y} \right) + S_L + S_B + S_K \quad (4)$$

where C represents the depth-averaged concentration of the water quality constituent in mg/l,  $E_x$  and  $E_y$  denote the longitudinal and lateral diffusion coefficients m<sup>2</sup>/s,  $S_L$  represents the loading rate due to direct and diffuse sources,  $S_B$  represents the loading rate at the boundaries (including U/S, downstream (D/S), benthic, and atmospheric sources), and  $S_K$  represents the total rate of kinetic transformation, where a positive value indicates a source and a negative value indicates a sink.

### 2.3 Initial and Boundary Conditions

Initial conditions consist of the constituents' concentrations at the simulation's start. In dynamic simulations that necessitate a transient concentration response, it is imperative that the initial concentrations employed accurately match the actual values at the beginning of the simulation (Wool et al., 2006). The value of initial conditions is entered for each segment via segment data entry. Fig. 2 shows the water quality constituents' D/S and U/S as boundary conditions.





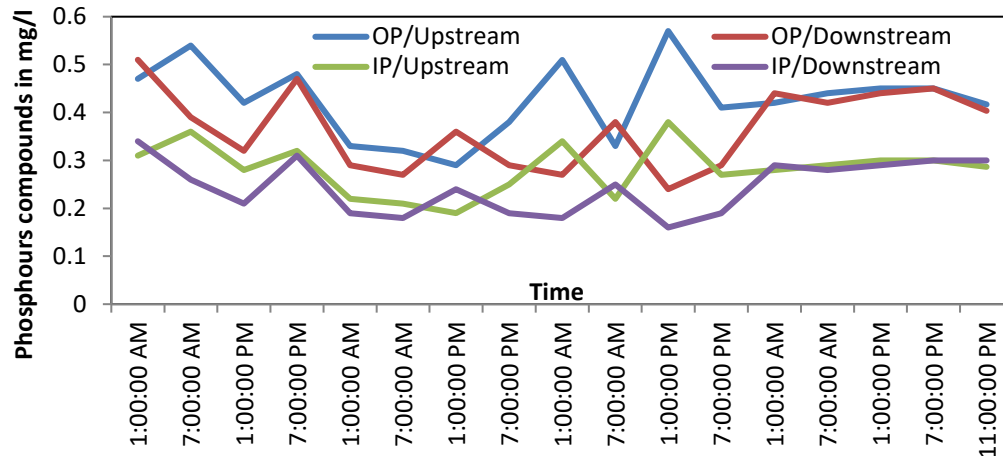


**Figure 2.** U/S and D/S boundary conditions of the water quality constituents during the simulation period (23-26), Aug. 2022

## 2.4 Construction Procedures

A proposed regulator is fixed at a desired location in a 2D model by drawing a profile line. Then, all characteristics and design parameters can be interred throughout the connection data editor. The figure shows that the regulator had an uncontrolled spillway of 100m X 1.5m with a 1.5 m crest level on the center of the regulator and eight sluice gates of 3 X 15 m.

## 3. RESULTS AND DISCUSSION

### 3.1 Results of Flood Control Events

Since the Arabian Gulf is the only water outlet in Iraq, and for Basrah governorate to benefit from maritime traffic from the available ports, including the port of Abu Flus, the appropriate location is near the port of Abu Flus, station 100+000m from the (U/S) end, which is located near Jeykor District north of Abu Flus port. The expected discharge of the flood situation is about 1650 m<sup>3</sup>/s; this discharge value is determined based on the probability of the maximum safe flood discharge for different return periods (100, 200, and 500 years) of the main tributaries of SAR. According to the Study of Strategy for Water and Land Resources in Iraq (**Ministry of Water Resources, 2014**), the Euphrates and Tigris rivers have average discharges of 400m<sup>3</sup>/s and 150m<sup>3</sup>/s, respectively (**Ministry of Water Resources, 2014**). Additionally, Al Karun and Al-Sweeb had discharges of 800m<sup>3</sup>/s and 300m<sup>3</sup>/s (MOWR) (**Ali and Al Thamiry, 2021**). If the contribution of Al Karun River is excluded according to Iran's water policy, the maximum discharge will be 850m<sup>3</sup>/s.

In the first, a maximum safe flow at the U/S end (850 m<sup>3</sup>/s), according to (**Ali and Thamiry, 2023**), was adopted, and the model was run without the construction of the regulator. The results stated that SAR can regulate this discharge, as shown in **Fig. 3**, where an overflow on the river's bank isn't happening.

Now, it should consider the effect of regulator construction on the river's capability to contain this flow condition. So, the model was run with several scenarios for the regulator operation to choose the best scenario that prevented the flood. The first one is based on U/S

water surface reference (U/S WS REF) where the gates opening are controlled depending on the upstream WSE. So, U/S WSE to open and close the gates was 1.5m and 0m, respectively. Another scenario depended on the time-series operation of the opening. This option gave the ability to make a schedule for opening and closing the gates. The scenario will close the gates during the flood period and open them during the ebb period, the movement of the tide out to the Arabian Gulf. Three-time series tables were adopted to check the optimal case, which gives a high water level without flooding. The rule based on which three different time series were made by identifying the gate opening height where it was 1 meter, 2 meters, and 3 meters for the time series 1, 2, and 3, respectively. A 2D unsteady model has simulated all scenarios, and the results of maximum WSE along the river are plotted in **Fig. 4**.

As illustrated in this figure, the lower WSE is achieved in the case without a regulator installed. This means losing the fresh water from the U/S feeder into the Arabian Gulf. In the case of installing the regulator with U/S water surface reference, it can be seen that the WSE significantly increased in the headwater side by 0.5 m above the current case (without regulator). In contrast, it is increased by about 1.0, 1.4, and 0.7 above the present case for time series reference operation systems 1, 2, and 3, respectively. But on the tail-water side, no significant variation can be noted.

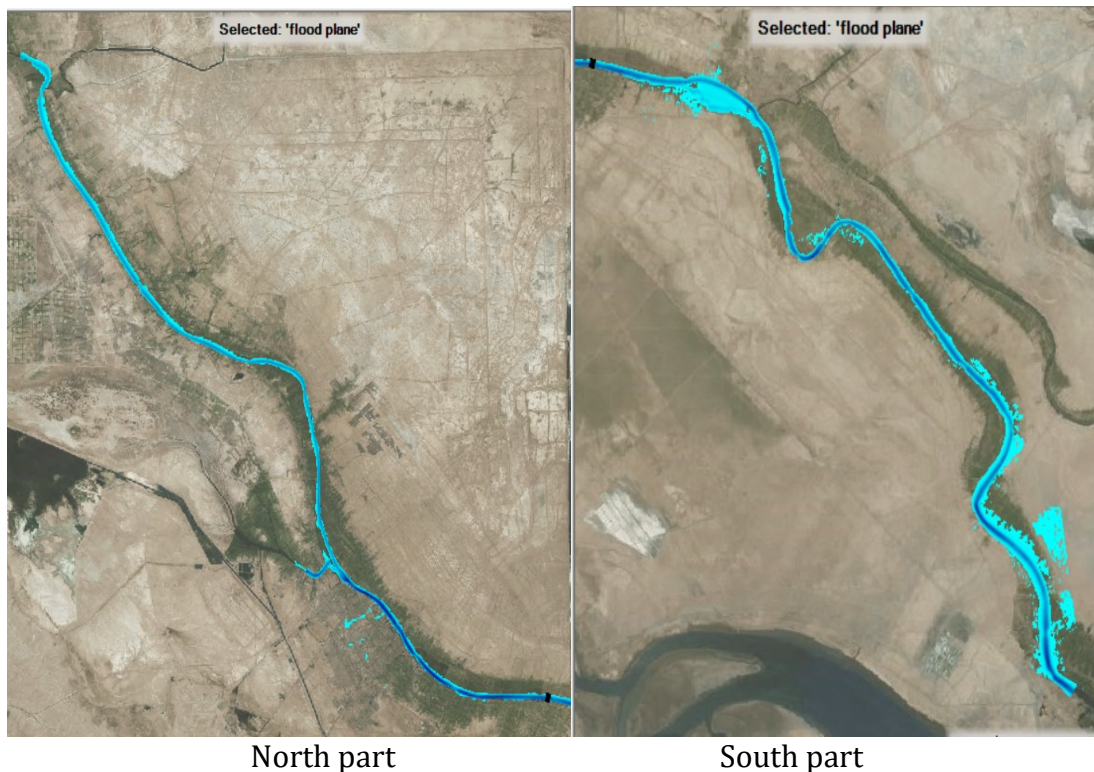


**Figure 3.** Study the area before installing the regulator with the maximum safe flow at the U/S end ( $850 \text{ m}^3/\text{s}$ ).

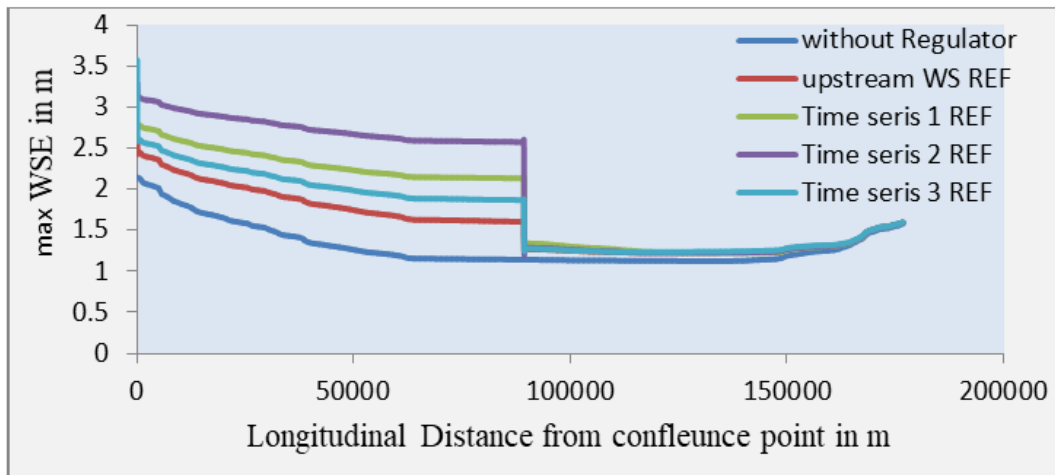
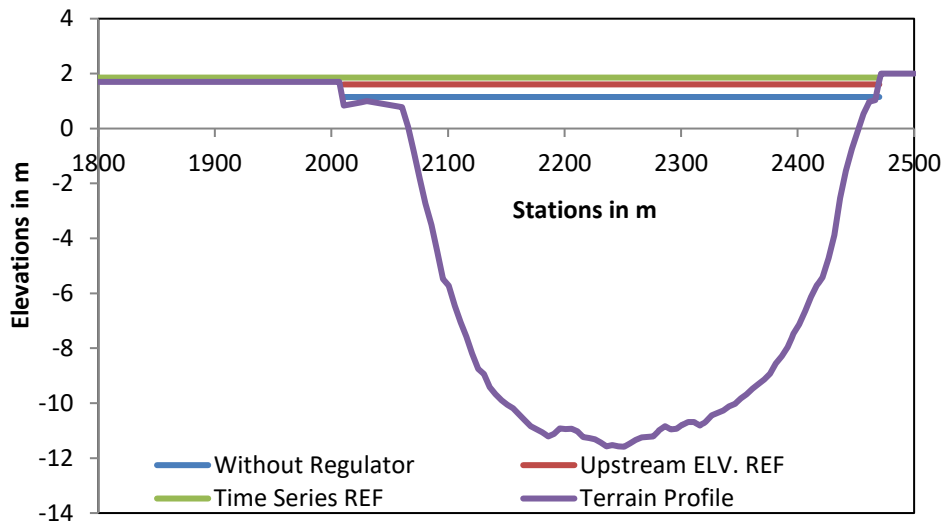


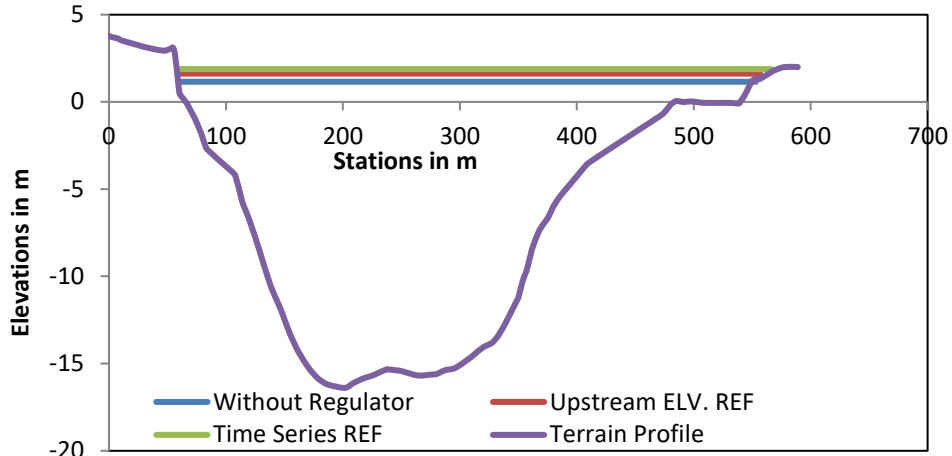
Figure 4. WSE throughout the different operation scenarios

To give a clear vision of whether the water level will rise in the main channel and cover the banks, the cross-section profiles at the different stations were made to choose an appropriate scenario that retains water without flooding the river’s banks. Fig. 5 shows the proposed regulator’s WSE profile across SAR U/S and D/S. The section on the D/S side was not overflowing on the banks for all scenarios, as in Fig. 5C and Fig. 5D. An alert is noted in the section located at 4000 m U/S of the regulator for the time series scenario. At the same time, the U/S WS REF gives a safe water level (Figs. 5A and 5B). This result can be recognized as shown in Fig. 6. According to the provided data, it can be inferred that the U/S ELV. REF scenario exhibits a higher level of safety concerning flooding when compared to the time series scenario.

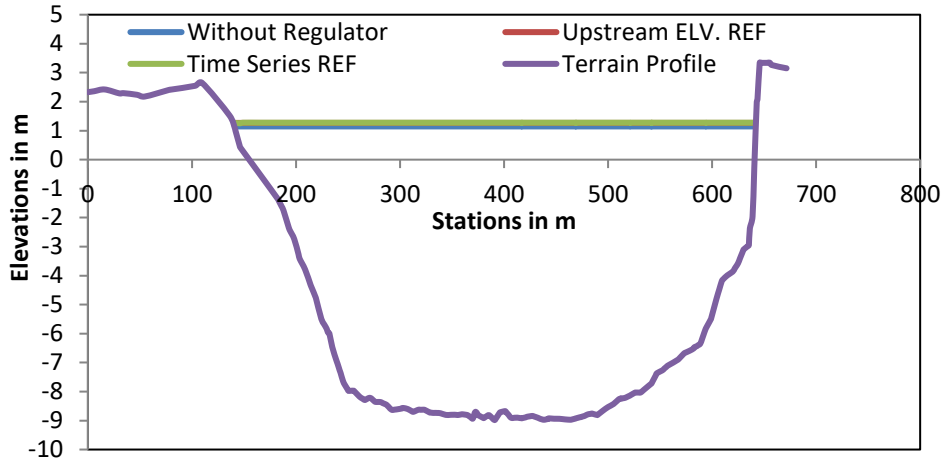


A) WSE at 4000 m U/S of the regulator

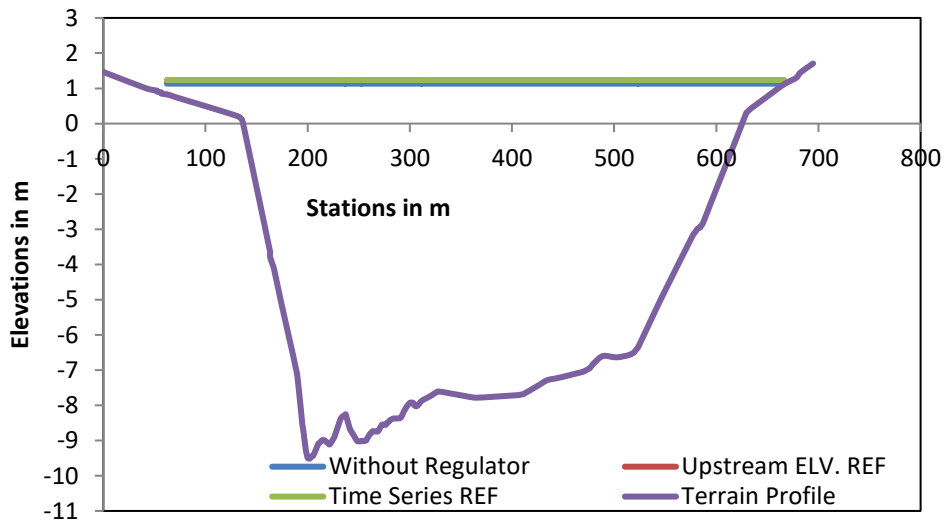




B) WSE at 16000 m U/S of the regulator

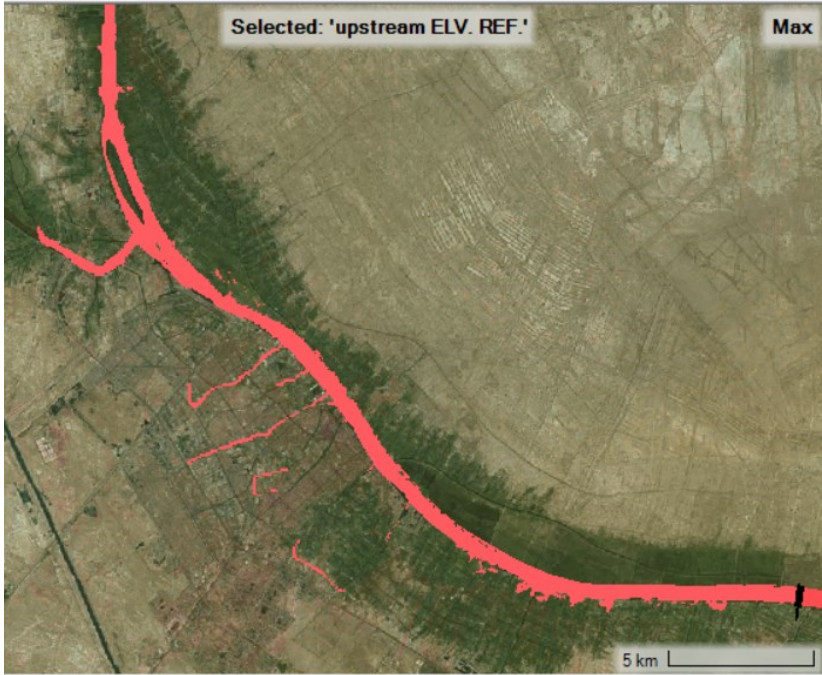


C) WSE at 3000 m D/S of the regulator

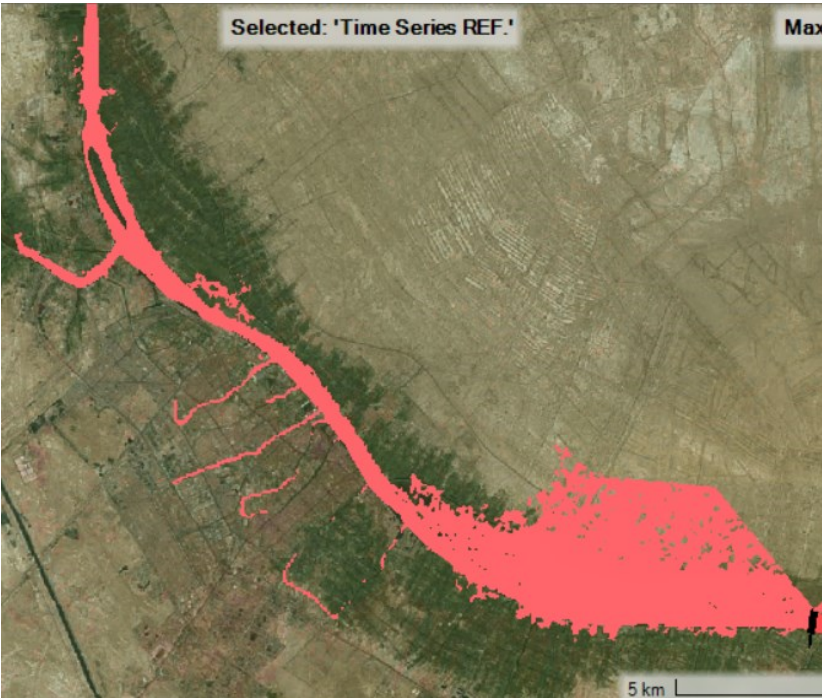


D) WSE at 28000 m D/S of the regulator

Figure 5. The cross-section profiles of WSE at different stations



A) U/S ELV. REF scenario



B) Time series REF scenario

Figure 6. The flood plain profiles of WSE in different scenarios

### 3.2 Results of Water Quality Control Events

After choosing the regulator site and choosing the best scenario for the gate opening operation, which ensures that no flooding occurs during maximum discharge ( $850 \text{ m}^3/\text{s}$ ), the next step is to study the impact of the regulator on the constituent's concentrations of water quality, especially in the Basrah Center. The model was executed, and its findings at the end of the simulation period were extracted for the eight EUTRO state variables as well as TDS and illustrated in graphs from **Fig. 7** to **Fig. 15**.

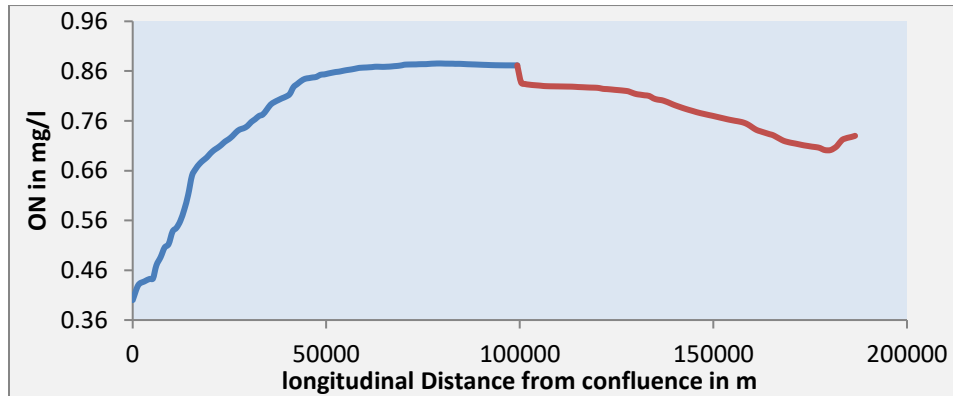


**Figure 7.** ON distribution along SAR after regulator construction

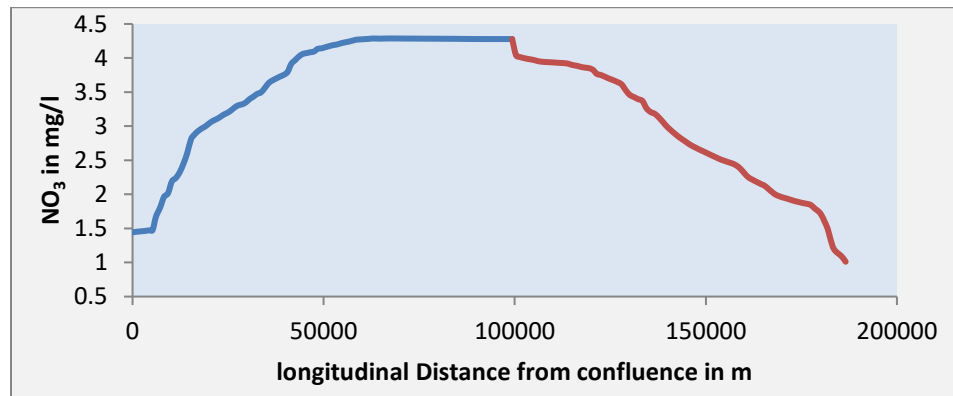


**Figure 8.** NO<sub>3</sub> distribution along SAR after regulator construction

In these Figs., the blue line signifies the U/S side of the regulator, while the red line signifies the D/S side. After studying these figures, the following points can be seen: the concentration of ON, NO<sub>3</sub>, NH<sub>3</sub>, OP, IP, and CBOD on the regulator U/S side was larger than on the regulator D/S side. So, the regulator has a negative impact on these water quality parameters in Basrah Center. The concentration of DO on the regulator U/S was smaller than on the regulator D/S. So, the regulator has a negative impact on this water quality parameter in Basrah Center. The concentration of PHYTO and TDS on the regulator U/S was smaller than on the regulator D/S. So, the regulator has a positive impact on these water quality parameters in Basrah Center.

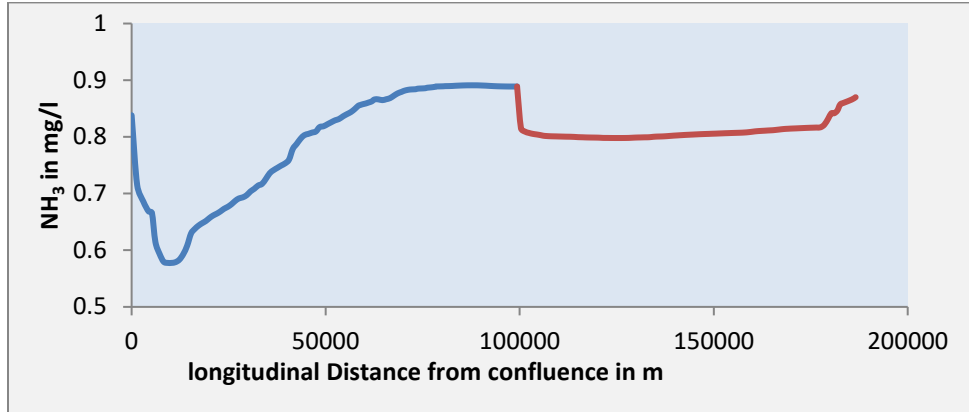


Figure 9. NH<sub>3</sub> distribution along SAR after regulator construction

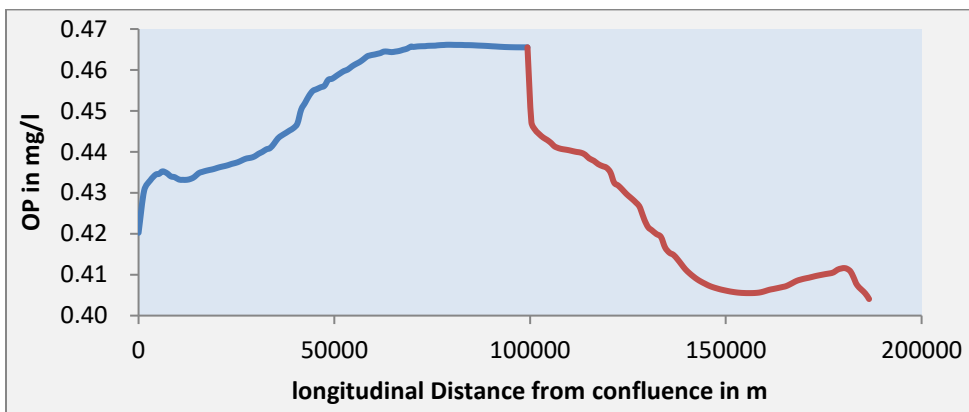


Figure 10. OP distribution along SAR after regulator construction

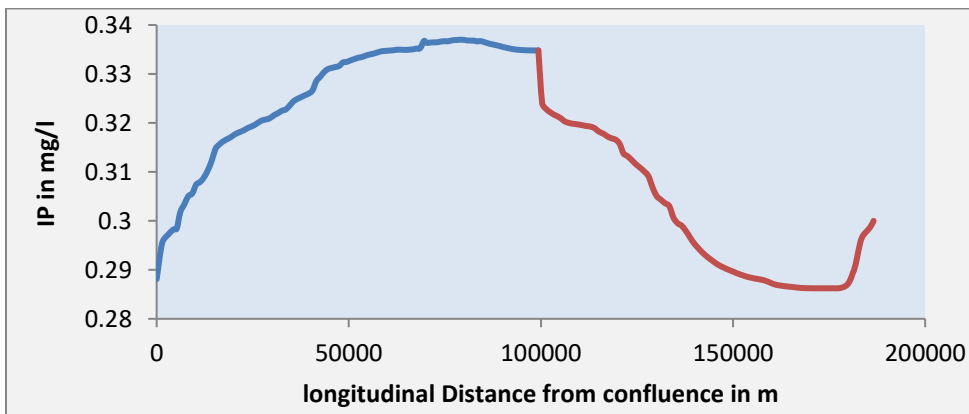


Figure 11. IP distribution along SAR after regulator construction

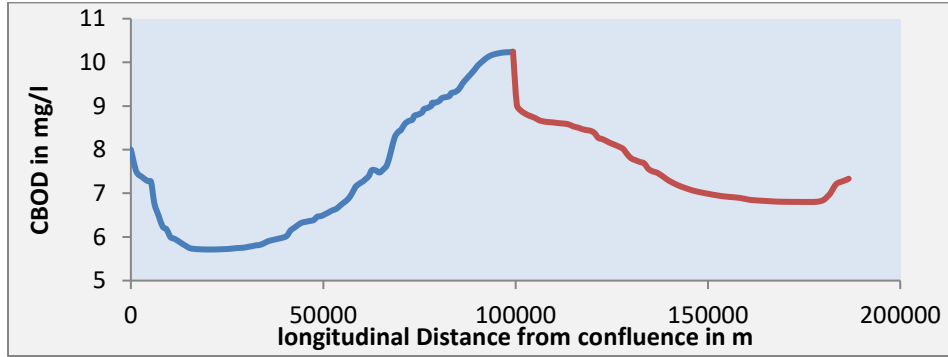


Figure 12. CBOD distribution along SAR after regulator construction

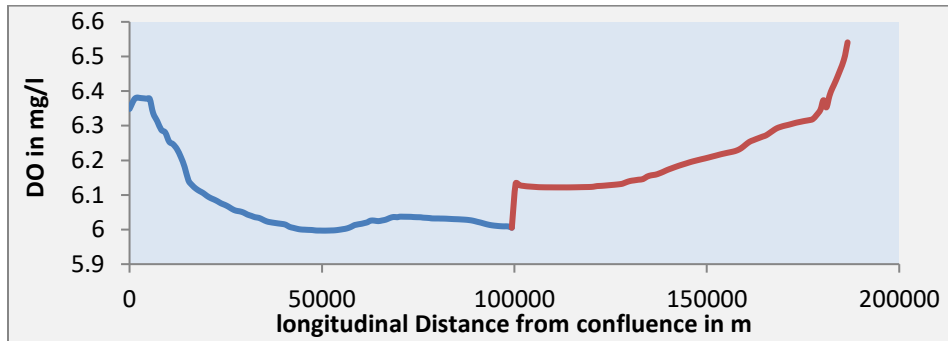


Figure 13. DO distribution along SAR after regulator construction

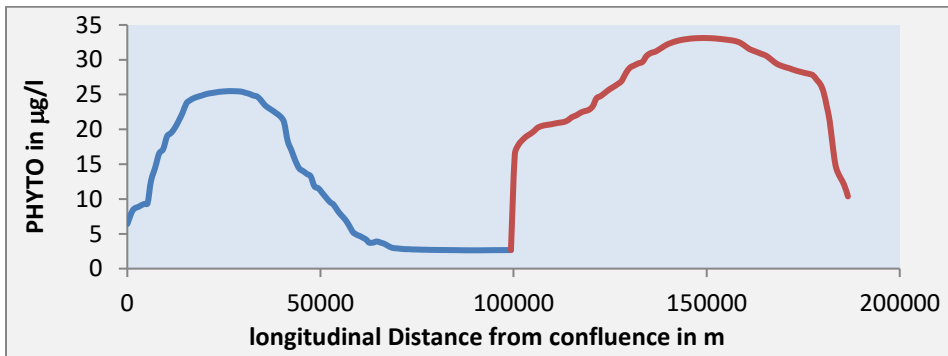


Figure 14. PHYTO distribution along SAR after regulator construction

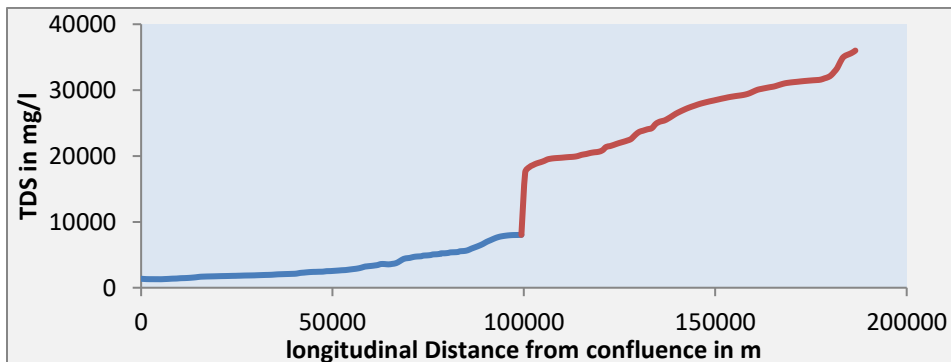


Figure 15. TDS distribution along SAR after regulator construction





**Table 1** was made to show a clear vision of the regulator's impact on pollutants as a removal percentage. The table shows the values of constituent concentration at station 100,000 metres, which is the same as the regulator construction site.

**Table 1.** Percentage removal of the constituents at the simulation end before and after construction of the regulator at station 100+000

| C1                     | C2                        | C3                       | C4              | C5                         | C6                         |
|------------------------|---------------------------|--------------------------|-----------------|----------------------------|----------------------------|
| Constituent            | Value before construction | Value after construction |                 | Removal %<br>(C2 - C3)/ C3 | Difference %<br>(C4-C3)/C4 |
|                        |                           | Just upstream            | Just downstream |                            |                            |
| NH <sub>3</sub> (mg/l) | 0.83                      | 0.89                     | 0.81            | -7.23                      | -9.88                      |
| NO <sub>3</sub> (mg/l) | 4.15                      | 4.3                      | 4.03            | -3.61                      | -6.70                      |
| IP (mg/l)              | 0.326                     | 0.335                    | 0.314           | -2.76                      | -6.69                      |
| PHYTO (µg/l)           | 13.5                      | 2.6                      | 16.4            | +80.74                     | +84.15                     |
| CBOD (mg/l)            | 9.13                      | 10.25                    | 9.01            | -12.27                     | -13.76                     |
| DO (mg/l)              | 6.16                      | 6.0                      | 6.14            | +2.60                      | +2.28                      |
| ON (mg/l)              | 0.84                      | 0.88                     | 0.82            | -4.76                      | -7.32                      |
| OP (mg/l)              | 0.45                      | 0.47                     | 0.43            | -4.44                      | -9.30                      |
| TDS (mg/l)             | 11560                     | 8025                     | 17523           | +30.58                     | +54.20                     |

The concentrations were recorded in the following cases: before the regulator (column C2), after the regulator construction/just U/S (column C3), and after the regulator construction/just D/S (column C4). The removal percent was calculated for each pollutant (column C5). The negative sign indicates the negative impact of the regulator on the pollutants (NH<sub>3</sub>, NO<sub>3</sub>, CBOD, ON, IP, and OP), while the positive removal percent indicates the positive effect of the regulator, except DO, as in the case of PHYTO and TDS, where the removal percent was +80.74 and +30.58, respectively. The table also shows the percentage difference in the pollutant concentrations between the two sides of the regulator, just U/S and D/S, in Column C6. These percentages showed a high restriction on the access of PHYTO and TDS to Basrah Center. While the blocking of water coming from the Gulf contributed to the increase of the rest of the pollutants inside the Basrah center.

There was a slight increase of ON, NO<sub>3</sub>, NH<sub>3</sub>, OP, IP, and CBOD and a decrease of DO due to trapping pollutants from the branches of rivers and stopping the cleaning process caused by the tides. This increase is expected, but it does not cause significant harm compared to the benefit expected from constructing the regulator due to the high decrease in TDS and PHYTO that it causes. TDS reduction is due to the increase in water volume and reduces the concentration U/S of the regulator. At the same time, the flow D/S reduction increases the TDS because of a higher concentration of the dissolved matter. In addition, there are efforts to prevent this pollution by establishing a system of conveyor pipelines to get rid of these pollutants. Therefore, it can be concluded that installing a regulator is a great benefit.

#### 4. CONCLUSION

The construction of a regulator on SAR is one of the solutions offered to preserve the freshwater from the Tigris River, reduce the salt intrusion from the Arabian Gulf, and control the levels within the province of Basrah. The research region encompasses the entirety of



the river's course, starting at the point where the Tigris and Euphrates Rivers meet in the Qurnah district and extending into the vicinity of the river's estuary.

It can be concluded from the results that a slight increase in ON, NO<sub>3</sub>, NH<sub>3</sub>, OP, IP, and CBOD and a decrease in DO were due to the effect of trapping pollutants coming out of the branches of rivers and stopping the cleaning process that was caused by the tides. This increase is expected, but it does not cause significant harm compared to the benefit expected from constructing the regulator due to the high decrease in TDS and PHYTO that it causes. The TDS reduction is due to increased water volume and decreased concentration upstream of the regulator. At the same time, the reduction in the downstream flow increases the TDS due to the presented higher concentration of the dissolved matter. In addition, there are government efforts to prevent this pollution by establishing a system of conveyor pipelines to get rid of these pollutants. Therefore, it can be concluded that installing a regulator is of great benefit.

## NOMENCLATURE

| Symbol    | Description                                                                   | Symbol                              | Description                                                      |
|-----------|-------------------------------------------------------------------------------|-------------------------------------|------------------------------------------------------------------|
| A         | Area, m <sup>2</sup> .                                                        | S <sub>L</sub>                      | Direct and diffuse loading rate, mg/l                            |
| C         | Concentration of a vertically averaged of the water quality constituent, mg/l | S <sub>B</sub>                      | Boundary loading rate, mg/l                                      |
| Ex and Ey | Longitudinal and lateral diffusion coefficients, m <sup>2</sup> /s            | S <sub>K</sub>                      | Total kinetic transformation rate, mg/l                          |
| g         | Gravitational acceleration, m/s <sup>2</sup>                                  | t                                   | Time, day                                                        |
| H         | Water depth, m                                                                | TDS                                 | Total Dissolved Solid, mg/l                                      |
| h         | Water surface elevation, m                                                    | u and v                             | Depth-averaged velocity components in the x and y direction, m/s |
| k         | Von Karman constant,                                                          | $v_{(\tau,xx)}$ and $v_{(\tau,yy)}$ | Horizontal eddy viscosity coeffi.in x and y directions           |
| Q         | Discharge value, m <sup>3</sup> /s                                            | $\tau_{(b,x)}$ and $\tau_{(b,y)}$   | Bottom shear stresses on the x and y directions                  |
| q         | Source/sink flux term, mg/l                                                   | $\tau_{(s,x)}$ and $\tau_{(s,y)}$   | The surface wind stress directions                               |
| R         | Hydraulic radius, m                                                           |                                     |                                                                  |

## Acknowledgements

This work was supported by the University of Basrah/Civil Engineering department and by HECRAS and WASP software.

## Credit Authorship Contribution Statement

Mohammed Jabbar Mawat: Writing – review & editing, Writing – original draft, Validation, Software, Methodology. Ahmed Naseh Ahmed Hamdan: Writing – review & editing, Software.



## Declaration of Competing Interest

The authors declare that they have no known competing financial interests or personal relationships that could have appeared to influence the work reported in this paper.

## REFERENCES

- Abd-El-Mooty, M., Kansoh, R., and Abdulhadi, A., 2016. Challenges of water resources in Iraq. *Hydrology Current Research*, 7(4), pp. 1-8. <https://doi.org/10.4172/2157-7587.1000260>.
- Abdo, K.M.M., 2014. Numerical modeling of free surface flows using depth averaged and 3D models. Thesis, University of South Carolina.
- Abdullah, A.D., Masih, I., van der Zaag, P., Karim, U.F., Popescu, I., and Al Suhail, Q., 2015. Shatt al Arab River system under escalating pressure: a preliminary exploration of the issues and options for mitigation. *International Journal of River Basin Management*, 13(2), pp. 215-227. <https://doi.org/10.1080/15715124.2015.1007870>.
- Abdullah, A.D., Gisen, J.I., van der Zaag, P., Savenije, H.H., Karim, U.F., Masih, I., and Popescu, I., 2016a. Predicting the salt water intrusion in the Shatt al-Arab estuary using an analytical approach. *Hydrology and earth system sciences*, 20(10), pp. 4031-4042. <https://doi.org/10.5194/hess-20-4031-2016>
- Abdullah, A.D., Karim, U.F., Masih, I., Popescu, I., and Van der Zaag, P., 2016b. Anthropogenic and tidal influences on salinity levels of the Shatt al-Arab River, Basra, Iraq. *International Journal of River Basin Management*, 14(3), pp. 357-366. <https://doi.org/10.1080/15715124.2016.1193509>
- Abdullah, A.D., 2017. Modelling approaches to understand salinity variations in a highly dynamic Tidal River: The case of the Shatt Al-Arab River. Netherlands. Thesis, Delft University.
- Al-Azzawi, S.N. and Khudair, K.M., 2001. A finite element model to simulate the hydrodynamics of Shatt Al-Basrah Canal and Khour Al-Zubair Estuary. *J Eng*, 7(2), pp.283-308.
- AL-Amiri, N.J., and Disher, M.A., 2020. Hydrochemical Study of Shatt al-Arab Water in Basra City. *Sys Rev Pharm*, 11(10), pp. 1162-1167. <http://dx.doi.org/10.5958/2394-448X.2021.00012.2>
- Al-Ansari, N., Ali, A., and Knutsson, S., 2014. Present conditions and future challenges of water resources problems in Iraq. *Journal of Water Resource and Protection*, 6(12), pp. 1066-1098. <http://dx.doi.org/10.4236/jwarp.2014.612102>
- Al-Asadi, S., and Abdullah, S., 2015. Estimating the minimum amount of the net discharge in Shatt Al-Arab River (South of Iraq). *Adab Al-Basrah*(72). pp. 285-314
- Al-Asadi, S.A., 2017. The future of freshwater in Shatt Al-Arab River (Southern Iraq). *J Geogr Geolo*, 9(2), pp. 24-38. <https://doi.org/10.5539/jgg.v9n2p24>
- Al-Asadi, S.A., Al-Qurnawi, W.S., Al Hawash, A.B., Ghalib, H.B., and Alkhelifa, N.H.A., 2020. Water quality and impacting factors on heavy metals levels in Shatt Al-Arab River, Basra, Iraq. *Applied Water Science*, 10(5), pp. 1-15. <https://doi.org/10.1007/s13201-020-01196-1>



- Al-Asadi, S.A., and Alhello, A.A., 2019. General assessment of Shatt al-Arab river, Iraq. *International Journal of Water*, 13(4), pp. 360-375. <https://dx.doi.org/10.1504/IJW.2019.106049>
- Al-Asadi, S.A., Alhello, A.A., Ghalib, H. B., Muttashar, W. R., and Al-Eydawi, H. T., 2022. Seawater intrusion into Shatt Al-Arab River, Northwest Arabian/Persian Gulf. *Journal of Applied Water Engineering and Research*, pp. 1-14. <https://doi.org/10.1080/23249676.2022.2113460>
- Al-Imara, F., Al-Shawi, I., and Al-Hwaichim, I., 2013. Ecological survey of some environmental factors and discharge of the Shatt Al-Arab estuary 1977-2012. *INOC-IIUM-International Conference on Oceanography & Sustainable Marine Production: A Challenge of Managing Marine Resources under Climate Change*, ICOSMaP, Kuantan-Malaysia.
- Ali, A.A., and Al Thamiry, H.A., 2021. Controlling the Salt Wedge Intrusion in Shatt Al-Arab River by a Barrage. *Journal of Engineering*, 27(12), pp. 69-86. <https://doi.org/10.31026/j.eng.2021.12.06>
- Ali, A.A., and Thamiry, H.A.A., 2023. Evaluation of the capability of Shatt Al-Arab River to control flood discharge. *AIP Conference Proceedings*, 2651, pp. 1-13. <https://doi.org/10.1063/5.0107121>.
- Alkanany, F.N., Rasheed, B.A., and Khudiar, M.M., 2017. Determination of bacterial contamination and some chemical parameters in Basrah Governorate Rivers. *Journal of Pharmaceutical, Chemical and Biological Sciences*, 5(2), pp. 118-124.
- AlKhafaji, H., Muttashar, W.R., and Al-Mosawi, W.M., 2023. Proposing an inflatable rubber dam on the Tidal Shatt Al-Arab River, Southern Iraq. *Journal of the Mechanical Behavior of Materials*, 32(1), pp. 1-8. <https://doi.org/10.1515/jmbm-2022-0201>
- Francesco Ambrosi, V.S., Paolo Benetazzo, Tina Cydzik, Andrea Scarinci, Paolo Mastrocola, Sami Ouechtati. 2014. Strategy for Water and Land Resources in Iraq.
- Hamdan, A., Dawood, A., and Naeem, D., 2018. Assessment study of water quality index (WQI) for Shatt Al-arab River and its branches, Iraq. *MATEC Web of Conferences* 162, pp. 1-7. <https://doi.org/10.1051/mateconf/201816205005>.
- Hamdan, A.N.A., Abbas, A.A., and Najm, A.T., 2019. Flood hazard analysis of proposed regulator on Shatt Al-Arab River. *Hydrology*, 6(3), pp. 80-99. <https://doi.org/10.3390/hydrology6030080>.
- Krenkel, P., 2012. *Water quality management*. 1<sup>st</sup> Edition.
- Lafta, A.A., 2022. Investigation of tidal asymmetry in the Shatt Al-Arab river estuary, Northwest of Arabian Gulf. *Oceanologia*, 64(2). pp. 376-386. <https://doi.org/10.1016/j.oceano.2022.01.005>
- Lateef, Z.Q., Al-Madhhachi, A.S.T., and Sachit, D.E., 2020. Evaluation of water quality parameters in Shatt Al-Arab, Southern Iraq, using spatial analysis. *Hydrology*, 7(4), pp. 79-111. <https://doi.org/10.3390/hydrology7040079>
- Mawat, M.J., and Hamdan, A.N.A., 2023a. Integration of numerical models to simulate 2D hydrodynamic/water quality model of contaminant concentration in Shatt Al-Arab River with WRDB calibration tools. *Open Engineering*, 13(1), pp. 1-17. <https://doi.org/10.1515/eng-2022-0416>



- Mawat, M.J. and Hamdan, A.N.A., 2023b. Simulation of 2D depth averaged saint Venant model of Shatt Al Arab river south of Iraq. *International Journal of Design and Nature and Ecodynamics*, 18(3), pp.583-592. <https://doi.org/10.18280/ij dne.180310>
- Ministry of Water Resources, 2014. The Study of Strategy for Water and Land Resources in Iraq, (SWLRI), , Baghdad, Iraq.
- Mohamed, A.R.M., and Abood, A.N., 2017. Ecological health assessment of the Shatt Al-Arab river, Iraq. 6(10), pp. 01-08.
- Mohammed, A. A., and Al Chalabi, A. S., 2022. Environmental impact assessment study for Shatt Al-Arab River receiving industrial wastewater. *Basrah Journal for Engineering Sciences*, 22(1). pp. 93-98. <http://dx.doi.org/10.33971/bjes.22.1.11>
- Mujtaba, A.T.A., Al-Nagar, G.A., and Al-Imarah, F.J.M., 2021. Cluster analysis for classification water quality of Shatt Al-Arab river. *International Journal of Aquatic Science*, 12(2). pp. 3814-3822.
- Munoz, D.V.H., 2017. Investigation of floodwave propagation over natural bathymetry using a three-dimensional numerical model. Thesis, The University of Iowa. <https://ir.uiowa.edu/etd/5948>
- Najm, A.T., 2017. Applications of two-dimensional surface flow modelling for Shatt AL- Arab River. Thesis, University of Basrah.
- Wool, T., Ambrose Jr, R.B., Martin, J.L., and Comer, A., 2020. WASP 8: The next generation in the 50-year evolution of USEPA's water quality model. *Water*, 12(5), pp. 1398-1430. <https://doi.org/10.3390/w12051398>
- Wool, T.A., Ambrose, R.B., Martin, J.L., Comer, E.A., and Tech, T., 2006. Water quality analysis simulation program (WASP). *User's manual, Version, 6*.
- Yaseen, B.R., Al Asaady, K.A., Kazem, A.A., and Chaichan, M.T., 2016. Environmental impacts of salt tide in Shatt al-Arab-Basra/Iraq. *IOSR Journal of Environmental Science, Toxicology and Food Technology*, 10(1-2), pp. 35-43.



## تخمين تأثير مقترح بناء ناظم على جودة مياه نهر شط العرب-العراق

محمد جبار موات<sup>\*</sup>، احمد ناصح احمد حمدان

قسم الهندسة المدنية، كلية الهندسة، جامعة البصرة، البصرة، العراق

### الخلاصة

يجري نهر شط العرب ، في جنوب العراق ، جنوباً شرقاً عبر مدينة البصرة ليصب في الخليج العربي. تتفرع من النهر ، خلال مساره ، سبعة جداول رئيسية وهي الجبيلة ، المفتية ، الرباط ، الخندق ، العشار ، الخورة ، والسراجي ، حيث تتأثر جميعاً بظاهرة المد والجزر . أثر التغير في الوضع الهيدرولوجي لنهر شط العرب على مدى العقد الماضي سلبا على جودة مياه النهر. حيث عادة ما يتم طرح مياه الصرف الصحي المنزلية ومياه الصرف الصناعية بشكل مباشر أو غير مباشر الى النهر. شملت الدراسة مجرى النهر بأكمله من التقاء نهري دجلة والفرات في منطقة القرنة إلى بالقرب من المصب في مدينة الفاو. تم استخدام نهر شط العرب في نمذجة مقترح انشاء ناظم على النهر باعتبارها واحدة من الحلول المقدمة لمعالجة تدهور نوعية مياه النهر. اظهرت النتائج زيادة طفيفة في النيتروجين العضوي، النترات، الأمونيا، الفوسفور العضوي، الفوسفور غير العضوي، والطلب على الأكسجين الكيميائي الحيوي الكربوني بنسب (4.76, 3.61, 7.23, 4.44, 2.76, 12.27)% عالتوالي وانخفاض الاوكسجين المذاب بنسبة 2.6% كان بسبب احتجاز الملوثات التي تغذيها فروع الأنهار وتوقف عملية التنظيف التي تسببها ظاهرة المد والجزر. من المتوقع حدوث هذه الزيادة. هذه الزيادة لا تسبب ضرراً كبيراً مقارنة بالفائدة المتوقعة من بناء الناظم نتيجة الانخفاض الكبير في إجمالي المواد الصلبة الذائبة بنسبة (30.58)% والعوالق النباتية بنسبة (80.7)%. بالإضافة إلى ذلك ، يمكن منع هذا التلوث من خلال إنشاء نظام من خطوط الأنابيب الناقلة للتخلص من هذه الملوثات. لذا استنتج أن هناك فائدة كبيرة لإنشاء ناظم.

الكلمات المفتاحية: برنامج HEC-RAS ، ناظم مقترح ، نمذجة نهر شط العرب ، جودة المياه.